AIMS Geosciences

AIMS Geosciences, 3 (3): 327-351
DOI: 10.3934/geosci.2017.3.327
Received date 04 March 2017
Accepted date 20 July 2017
Published date 27 July 2017

http://www.aimspress.com/journal/geosciences

Research article

Evaluating the Impacts of Climate Change on Soil Erosion Rates in Central Mexico

Santos Martínez-Santiago [1], Armando López-Santos [1,*], Guillermo González-Cervantes [2] and Gerardo Esquivel-Arriaga [2]

[1] Graduate Program in Recursos Bióticos y Medio Ambiente de Zonas Áridas, Unidad Regional Universitaria de Zonas Áridas, Universidad Autónoma Chapingo. Km. 40 Rd. Gómez Palacio-Chihuahua. Bermejillo, Dgo. México, ZC 35230

[2] INIFAP-CENID-RASPA, Km 6.5 margen derecha canal Sacramento, Gómez Palacio, Durango, México, 35140

* **Correspondence:** Email: alopez@chapingo.uruza.edu.mx; Tel.: +52-872-776-0160; Fax: +52-872-776-0043.

Abstract: Although water-eroded soil (*WES*) resulting from human activities has been recognized as the leading global cause of land degradation, the soil erosion risks from climate change are not clear. Studies have reported that *WES* is the second most significant cause of soil loss in Mexico, and its future trajectory has not been sufficiently evaluated. The aims of this study are to 1) determine the impacts of climate change on *WES* and its distribution for the State of Aguascalientes, Mexico, and to 2) compare the present and future soil loss rates for the study unit (SU). The State of Aguascalientes is located in the "Region del Bajio." The impact of climate change on *WES* was evaluated using the near-future divided world scenario (A2) presented in the IPCC Fourth Assessment Report. Daily temperature and precipitation data from 18 weather stations were downscaled to model historic laminar water erosion (*HLWE*) and changes therein in the A2 near-future scenario for 2010–2039 (LWE_{ScA2}). Due to future changes in mean annual

rainfall (*MAR*) levels, a change in the LWE_{ScA2} of between 1.6 and 8.9% could result in average soil losses up to 475.4 t ha^{-1} yr^{-1}, representing a loss of slightly more than a 30-mm layer of mountain soil per year. The risk zones, classified as class 4 for *LWE*, are located to western of the State in part of municipalities of Calvillo, Jesus María, San José de Gracia y Cosio, where there are typical hills and falls with soil very sensitive to rain erosion.

Keywords: erosion rate; land degradation; land use; climate change scenarios; risk; adaptation

1. Introduction

In many countries with complex socioenvironmental and economic problems [1–4], water-eroded soil (*WES*) is considered to be the main cause of land degradation [5–7]. Under natural conditions, each millimeter of eroded soil produces lower levels of biological wealth [8,9], whereas in a farming system, this measure is related to a permanent need for increased amendments to crops to obtain the highest price of goods [1,10]. For example, Gao et al. [10] argue that when black soils in northeastern China were eroded to a depth of 0.4 m, soybean production decreased by nearly 10%.

Currently, 56% of the 3.5 billion of hectares of land in the world present signs of degradation, affecting approximately 1.5 billion people living in these areas [2,5,11]. Stavi and Lal [2] reported on historical changes in potential erosion levels occurring over the last century (1901 to 1980) and maintained that such changes have been caused by an increase in human activities such as deforestation, land use intensification and land use change, with up to 60% of these land degradation trends detected across all continents except for Europe.

Other reports [4,12] have estimated soil losses ranging from 24 to 75 billion tons of fertile soil. For example, Wang et al. [4] reported that arable land has been lost due to soil erosion at a rate of more than 10 million ha per year.

In Mexico, an average estimate based on several reports [13–15] shows that 69.7% (1354 thousand of km^2) of the country's land (1949.8 thousand of km^2) presents some degree of degradation in the soil component of land, with *WES* representing the highest proportion with 25.4% (494 thousand of km^2), followed by chemical degradation and wind erosion measured at 20.1% (390 thousand of km^2) each, and finally physical degradation at 4.1% (79 thousand of km^2).

Climatic variability has worsened in recent years, affecting many countries, including Mexico [16]. Mexico's susceptibility to water erosion hazards is high because approximately half of the country's territory (42.2%) has a slope greater than three degrees. This topographic feature, along with the inadequate management of forests, agriculture and grazing, promotes the generation of runoff, which erodes topsoil [13,17,18].

The State of Aguascalientes is currently suffering from a critical loss in natural resource quality. Since the start of the previous decade, it has been officially reported that [19,20] approximately 2853 km^2 of land has shown a certain degree of degradation, representing 51% of the state's territory (5621 km^2), with 1307 km^2 exhibiting WES, representing 46% (1307/2853 km^2) of the affected area and 23.2% (1307/5621 km^2) of the territory of the state. In a national ranking of states with the highest degrees of degradation from WES, Aguascalientes is ranked fifth after Guerrero (31.8%), Michoacán (27.1%), Mexico (25.7%) and Jalisco (25.3%).

Generally, the following three forms of soil erosion occur in Mexico: i) land deformation (26,604.3 km^2 (1.4%)); ii) topsoil loss (200,039.7 km^2 (10.5%)); and iii) off-site soil loss (613.1 km^2 (0.03%)). For Aguascalientes, the third form has not been measured (iii), but evidence shows that the first (i) [21] and second (ii) processes are more significant, appearing over 199.9 km^2 (3.7%) and 1,106.7 km^2 (20.5%) of the territory, respectively [14,16].

Land deformations due to land subsidence, surface faults and surface cracks are a typical problem related to groundwater extraction, and for unconsolidated alluvial sediments underground, both factors have been described by Aranda-Gómez [22] and Pacheco-Martínez et al. [21] in reference to the Aguascalientes Valley.

Estimating topsoil loss as laminar soil loss, Sun et al. [1] argue that the Universal Soil Loss Equation (USLE), Revised Universal Soil Loss Equation (RUSLE), Erosion Productivity Impact Calculator (EPIC) and Water Erosion Prediction Project (WEPP) are accepted methods for estimating soil erosion rates. The USLE, or the RUSLE model, is a universally accepted method that can be used as the best fitted model for monitoring rates. The applicability of this model has been proven over recent decades, and it is now widely accepted [1,6,23–25].

In reference to Mexico, some studies [23,24] have reported soil erosion rates above those that have been previously indicated. For example, Montes-León et al. [24] used the USLE model for hydrologic region 12 in Lerma-Santiago, Aguascalientes and reported potential extreme soil losses at rates of >250 t ha^{-1} yr^{-1} without considering the effects of climate change. Other studies [26–28] based on the same model (USLE) have reported higher rates than this.

The aims of this research are 1) to determine the effects of climate change on WES and the distribution thereof within the State of Aguascalientes, Mexico, using the near-future divided world scenario (A2) drawn from the Intergovernmental Panel on Climate Change (IPCC) Fourth Assessment Report (AR4), and 2) to predict the future risks resulting from the deterioration of soil resources.

2. Brief Background on Climatic Change Scenarios

To improve our understanding of the complex relationships between the climate system, ecosystems, and human activities, the scientific community has developed scenarios that provide plausible accounts of how key socioeconomic and technological areas and environmental conditions

could be affected by greenhouse gas (GHG) emissions and climate change [29]. However, the implementation of these scenarios at the local level, which is of significance for vulnerability studies on climate change adaptation, represents a growing challenge [2,30].

The future climatic scenarios produced by Conde and Gay [31] present precipitation and temperature anomalies; these scenarios are the result of numerous experiments conducted based on the 23 Global Circulation Models (GCMs) proposed by the IPCC. In fact, this work constitutes the basis of the GHG emission trajectories [31,32]. These future climatic scenarios have the following characteristics: Scenario A1 assumes a very rapid rate of global economic growth, a doubling of the world population by mid-century, and the rapid introduction of new and more efficient technologies. This scenario is divided into three sub-scenarios that reflect three alternative directions for technological change: intensive fossil fuel use (A1FI), non-fossil energy use (A1T), and a balance between various energy sources (A1B). Scenario B1 describes a convergent world with the same population as that of A1 but with a more rapid evolution of economic structures toward a service and information economy. Scenario A2 describes a very heterogeneous world with strong population growth, slow economic development, and slow technological change.

The GHG emission assessment scenarios (A1B, A2, B2, and B1) show an approximately 3% reduction in annual rainfall levels, a nearly 1°C increase in the annual average temperature, and a 6°C temperature increase for the fall. The longest drought occurs from 2010–2039 and is centered on the fragile dry lands of northern Mexico [31–33].

3. Materials and Methods

3.1. Study unit

The State of Aguascalientes in Mexico is located in the central northern region (Figure 1a), covering a total area of 5621.5 km^2 and representing 0.3% of the national territory [34]. According to the INEGI [34], there are three main climates within this territory: arid (BS1kw), semiarid (BS1kw(w)) and subhumid (C(w0), C(w1)) (Figure 1b). In addition, this area presents a physiographic conformation that includes vast hills and plains, including the Sierra Madre Occidental, Mesa del Centro and Eje Neovolcanico, ranging from 1800 to 3050 masl (meters above sea level) (Figure 1c).

Based on the climate and physiography briefly described above (Figure 1), the soil, land use and vegetation features are described as follows. According to the WRBS (World Resources Base of Soils), Aguascalientes includes 10 of the 32 soil groups in the world. There are three main soil groups (Phaeozems, PH (31.58%), Leptosols, LP (21.36%) and Durisols, DU (18.89%)) that cover almost three-quarters of the territory of the state.

According to the INEGI [35], there are three forms of land use in Aguascalientes. The main land use covers approximately 2386.5 km^2 (42.5% of the state's land area) and is managed under rainfed (18.6%) and irrigated conditions (23.8%). The second land use involves secondary vegetation, covering 1193 km^2 (equivalent to 21.2%) and includes vegetation such as oak bushes (7.4%), natural grassland (4.1%), deciduous forest vegetation (5.1%) and scrubland (4.3%). Finally, primary vegetation occupies approximately 988.4 km^2 (representing 17.6% of the total surface) and includes oak and pine forest (7.2%), natural grassland (5.47%), scrubland (4.1%), and high-altitude moist evergreen and semi-deciduous forest (0.8%).

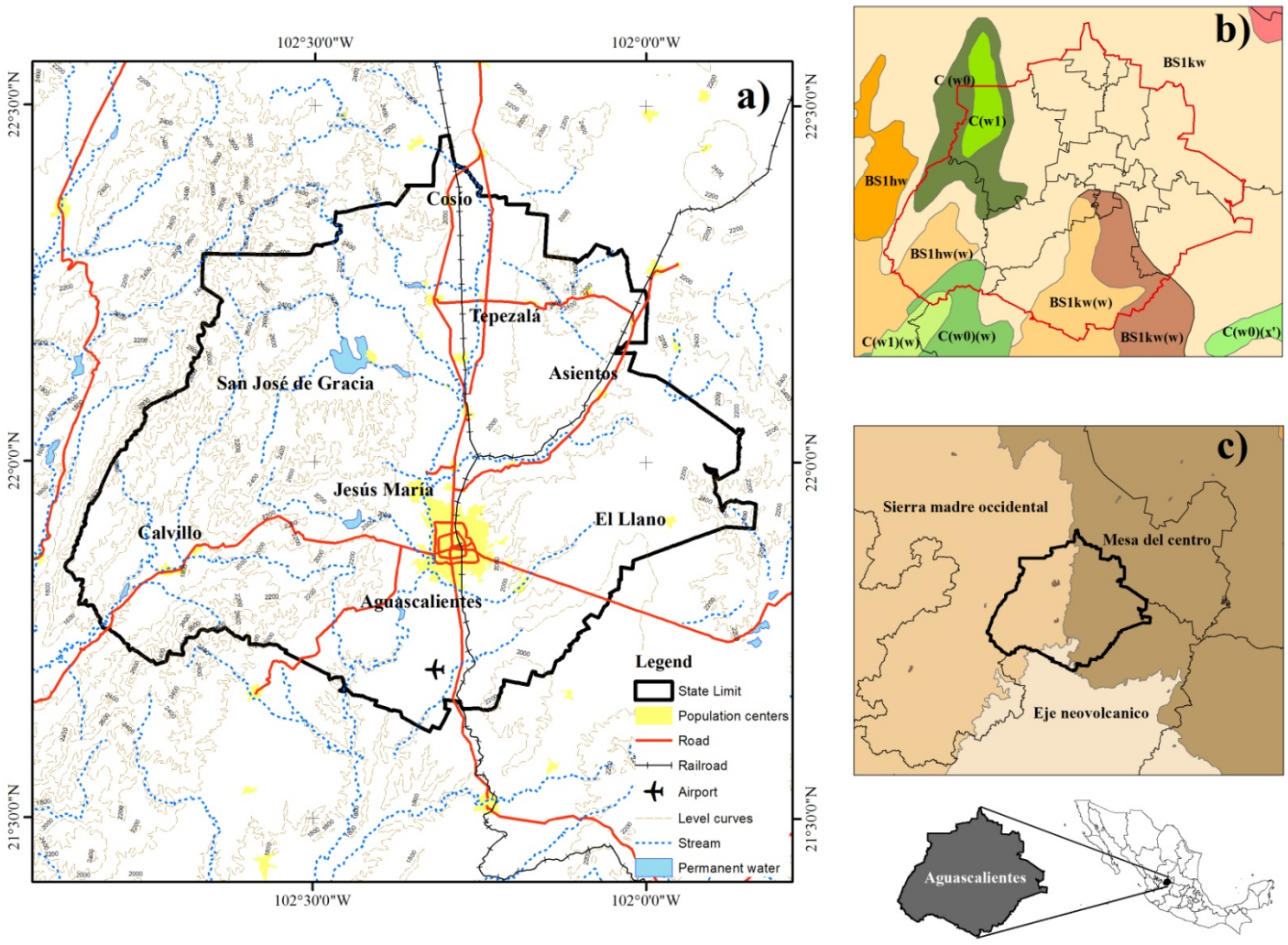

Figure 1. The location (a), climatic distribution (b), and physiography (c) of the State of Aguascalientes.

3.2. LWE calculation and modeling

The *LWE* calculation and modeling in this work is based on the methodology proposed by the SEDESOL-INE [36] for Land Use/Land Cover (LULC), which has been used in similar studies [37,38] to model the local effects of climate change in northern Mexico. From this same methodology, we used [36] as a reference for four probable classes of soil loss: 1) light, < 10 t ha^{-1} yr^{-1}; 2) moderate, 10-50 t ha^{-1} yr^{-1}; 3) high, 50-200 t ha^{-1} yr^{-1}; and 4) very high, > 200 t ha^{-1} yr^{-1}. The method employed is a function of the available humidity as a consequence of rain, and other factors were considered, as described below.

According to the climatology patterns briefly described above and the climatology dataset used, it is assumed that the dominant environmental process is related to the rain aggressiveness index (*RAI*) due to the dependence of this index on the mean annual rainfall (MAR), which determines the growth period (*GROPE*) for annual plants while also defining the humidity levels available to crops for planting, strong root formation and growth [39,40]. The number of days (d) for each climatological case are as follows [41]: 1–59 d (arid), 60-119 d (semiarid) and subhumid (120–179 d). Both indices are expressed as follows:

$$RAI = (1.244 \times GROPE) - 14.7875 \qquad \text{[Eq. 1]}$$

$$GROPE = (0.2408 \times MAR) - (0.0000372 \times MAR^2) - 33.1019 \qquad \text{[Eq. 2]}$$

Once the bioclimatic variables described above were calculated (Eq. 1 and Eq. 2), the *LWE* was determined from biophysical properties of anthropogenic influence (land use) for the study area, as shown below:

$$LWE = RAI \times CAERO \times CATEX \times CATOP \times CAUSO \qquad \text{[Eq. 3]}$$

where *CAERO* (Spanish acronym) is an index that defines a soil layer's susceptibility to environmental effects, such as rain or wind; *CATEX* (Spanish acronym) is an index associated with the outstanding properties of the same soil layer's texture and physical phase; *CATOP* (Spanish acronym) is an index related to landforms and dominant slope classes; and *CAUSO* (Spanish acronym) is an index related to soil uses and the dominant vegetation types.

3.3. Preparation of input variables for LWE calculation

The input variables for the *LWE* calculation shown in Eq. 3 were prepared from their original formats (*shp* and Geotiff) for processing using the raster calculator available through ArcGIS 10.1® (ESRI, Redlands, CA, USA) in the Spatial Analyst module. The primary steps of this procedure are as follows.

3.3.1. Vector dataset processing

The cartographic coverage used for Aguascalientes State involved modifying the attribute tables of vector datasets edited and distributed by the INEGI (F13–06, F13–09, F14–04 y F14–07) at a scale of 1:250,000. To create the CAERO and CATEX indices, edaphology set II [41] was used; for CAUSO, Land Use and Vegetation (LUV) set IV (INEGI, 2007b) was used.

From the original methodology (SEDESOL-INE, 1998), CAERO was defined from the soil properties described by Wischmeier and Smith [42], which have been used in several studies [43,37,38]. These properties correspond to the soil units and subunits of set I. Therefore, it was necessary to standardize these units with the groups and edaphological classifiers of set II (Table 1), which were based on the same WRBS classification published in 1998 [44] and were officially adopted for soils in Mexico in 2007.

Table 1. Homologation of the *CAERO* index between sets I and II of the edaphic coverage for the State of Aguascalientes.

Set I (code)	*CAERO*	*Set II (code)*
Xerosol (X), Yermosol (Y)	2	Calcisol (CL)
Planosol (W)	2	Planosol (PL)
Litosol (L)	2	Leptosol (LP)
Litosol (I)	2	Durisol (DU)
Kastanozem (K)	1	Kastanozem (KS)
Luvisol (L)	1	Luvisol (LV)
Regosol (R)	1	Regosol (RG)
Cambisol (B)	1	Cambisol (CM)
Fluvisol (J)	0.5–1.0	Fluvisol (FL)
Feozem (H)	0.5	Phaeozem (PH)

Source: "Guía de Interpretación Edafológica" from INEGI [45] set I, INEGI [46] set II and IUSS-WG-WRB [44].

In this same vector set (edaphology set II), the field corresponding to the texture and physical phase was extracted to create the *CATEX* index (Table 2) in a new attribute table representing the soil textural properties and physical phase to a depth of 0.3 m. This attribute table was converted to a raster layer as indicated in Eq. 3.

As noted above, the CAUSO index uses the vector dataset of LUV sets III and IV, with the first extending the reference for groups within each form of land use and the second representing the most recent data (Table 3).

Table 2. *CATEX* index according to soil textures for the State of Aguascalientes.

------- *INEGI*[a] -------		---------- *USDA*[b] ----------		
TCPP	Code	Textural group	Relative composition	CATEX[c]
Coarse	1	Sandy	≥ 65% of sand	0.2
Medium	2	Loamy	in equilibrium	0.3
Fine	3	Clayish	≥ 35% of clay	0.1
SPB	SPB	NA	Stone with diameter ≥ 7.5 cm	0.5

Source: [a]INEGI [47]; [b]USDA = United States Department of Agriculture; [c]SEDESOL-INE [36]; TCPP = Textural class and physical phase; SPB = Stony phase or burdensome; NA = Not applicable.

Table 3. *CAUSO* index defined for four vegetation types for the State of Aguascalientes.

---------- *LUV INEGI* ----------		--- *CAUSO*[c] ---	
Set III[a]	***Set IV***[b]	***LUV***	***Index***
Irrigated agriculture with a slight slope (0–2%)	Irrigated agriculture with a slight slope (0–2%)	Agriculture	0.8
Forests: pine, pine-oak, juniper low open, and oyamel	Forest: Conifers, cultivated, oak, mesophyll	Forest	0.1
Grassland: halophyte, natural, grassland-huizachal, cultivated rainfed grassland, induced rainfed agriculture, and secondary jungle vegetation	Grassland and induced vegetation	Grassland	0.12
Scrubs: submontane, crassicaule, desert micropyle, rosette, sarcocaulis, chaparral, gypsophila and halophytic vegetation including mesquite	Scrub	Scrubland	0.15

Source: [a]INEGI [48]; [b]INEGI [35]; [c]SEDESOL-INE [36]; LUV = Land use and vegetation.

3.3.2. Landform and slope class processing and preparation

The *CATEX* index was derived from a 30-meter resolution digital elevation map of Mexico [49]. The *CATOP* values were defined as a function of slope using three classes and three landforms, as shown in Table 4.

Table 4. *CATOP* Index defined for Aguascalientes State.

CATOP	Slope	Rank	Landform
0.35	A	0-8	Valleys, plains and plateaus with variation of 500 m
3.5	B	8-30	Hills and plateaus with variation of 500 to 750 m
11.0	C	>30%	Sierras and plateaus with variation of more than 750 m

Source: SEDESOL-INE [36]

3.4. Definitions of baseline climate data, homogenization and downscaling

3.4.1. Baseline climate data and homogenization

The baseline or reference year was set as 2010, and daily climatic data for temperature and rainfall were obtained from 18 National Weather Service (WS-NWS) weather stations, with 17 located in Aguascalientes and one located in Jalisco (Id-code: 14122). The WS selection criteria were as follows: 1) at least 30 years of climatic data; 2) database quality; and 3) proximity to the mesh resolution node (50 x 50 km) for climate change scenarios for Mexico (AR4). The first criterion used an average of 54 years of data. For the third criterion, the five nodes identified for this territory have the following locations (longitude, latitude): 1 (102.75, 22.25); 2 (102.25, 22.25); 3 (102.75, 21.75); 4 (102.25, 21.75); and 5 (101.75, 21.75). The quality levels were determined based on the RClimDex©, ver 1.0 daily climate database for homogenization (www.r-project.org), from which 27 indices were obtained for climatic change detection. We selected six key variables, as shown in Table 5.

3.4.2. Downscaling method

We used the LARS-WG (*Long Ashton Research Station Weather Generator*) downscaling method as a time stochastic weather generator (TSWG). The LARS-WG can simulate daily weather data variables based on the statistical characteristics of the observed data in one place. The LARS-WG was applied to the 18 WS-NWSs selected (Table 5). Using the LARS-WG, we obtained the synthetic series for climate change scenarios A2 and A1B for 2010–2039 for the same input variables based on the 15 general circulation models (GCMs) that were used for the IPCC AR4 [32].

The analysis of current and future climatic patterns to estimate the likely regional impacts of climate change was carried out using the Regionalized Climate Models for Mexico (RCMM) created by the UNAM Center for Atmospheric Sciences, which has a resolution of 2500 km^2 with nodes equidistant at 50 × 50 km (Figure 2).

Table 5. Selected nodes and weather stations and five climate indices for the State of Aguascalientes.

Node	*WS*	*WS*	*Location (lat/long)*		*masl*	*Range data*		*MAT*	*MAR*	*DDM*	*DRM*	*WR*	*R/T*
Num	*Code*	*Official name*	*---- dg ----*		*m*	*start*	*ny*	*°C*	*------- mm -------*			*%*	
1	1010	La Tinaja	22.164	102.554	2526	1963	47	16.7	647.9	5.3	159.3	7.2	38.8
	1021	Rancho Viejo	22.123	102.511	2127	1963	47	18.2	570.6	4.4	148.5	6	31.4
2	1008	Pto. de la Concepción	22.203	102.135	2323	1963	47	16.9	484.1	3.6	133.5	7.6	28.6
	1013	Mesillas	22.313	102.166	2021	1963	47	16.8	379.4	2.2	90.4	8	22.6
	1014	Pabellón-Campo Exp.	22.167	102.293	1934	1939	71	15.3	453.0	3	126.7	6.4	29.6
	1017	Presa Potrerillos	22.233	102.444	2172	1947	63	15.5	495.0	4.7	125.3	7	31.9
	1018	Presa Calles	22.141	102.415	2053	1939	71	16.4	478.3	2.8	119.8	6	29.2
	1019	Presa Jocoque	22.128	102.359	2006	1942	68	17.2	469.2	2	117.5	6	27.3
3	1011	Malpaso	21.860	102.664	1730	1950	60	20.7	556.0	2	141.9	5.3	26.9
	1012	Presa Media Luna	21.794	102.802	1589	1970	40	15.5	646.3	2.8	171	4.7	41.7
	1020	Presa la Codorniz	21.997	102.674	1850	1963	47	18.7	594.6	3.8	152.2	5.6	31.8
4	1004	Cañada Honda	22.001	102.199	1925	1970	40	17.3	486.3	2.7	119.2	6.7	28.1
	1005	Presa El Niagara	21.780	102.372	1844	1957	53	17.6	540.0	3	149.5	5.4	30.7
	1024	San Isidro	21.779	102.104	2004	1970	40	15.3	308.6	1.2	83.3	5.3	20.2
	1027	Venaderos	21.876	102.463	2026	1951	59	14.9	505.8	2.9	122.9	6	33.9
	1030	Aguascalientes	21.895	102.308	1889	1948	62	16.1	501.8	2.6	127	5.5	31.2
	14122	San Bernardo	21.632	102.391	1085	1942	68	15.6	540.1	1.4	142.9	4.5	34.6
5	1015	Palo Alto	21.916	101.969	2037	1968	42	17.1	505.5	3.4	120.4	6.6	29.6

WS = Weather station; masl = meters above sea level; ny = number of years until 2010; DDM = Data for the driest month; DRM = Data for the rainiest month; WR = Winter rainfall; R/T = Annual rain and temperature index; dg = decimal degrees

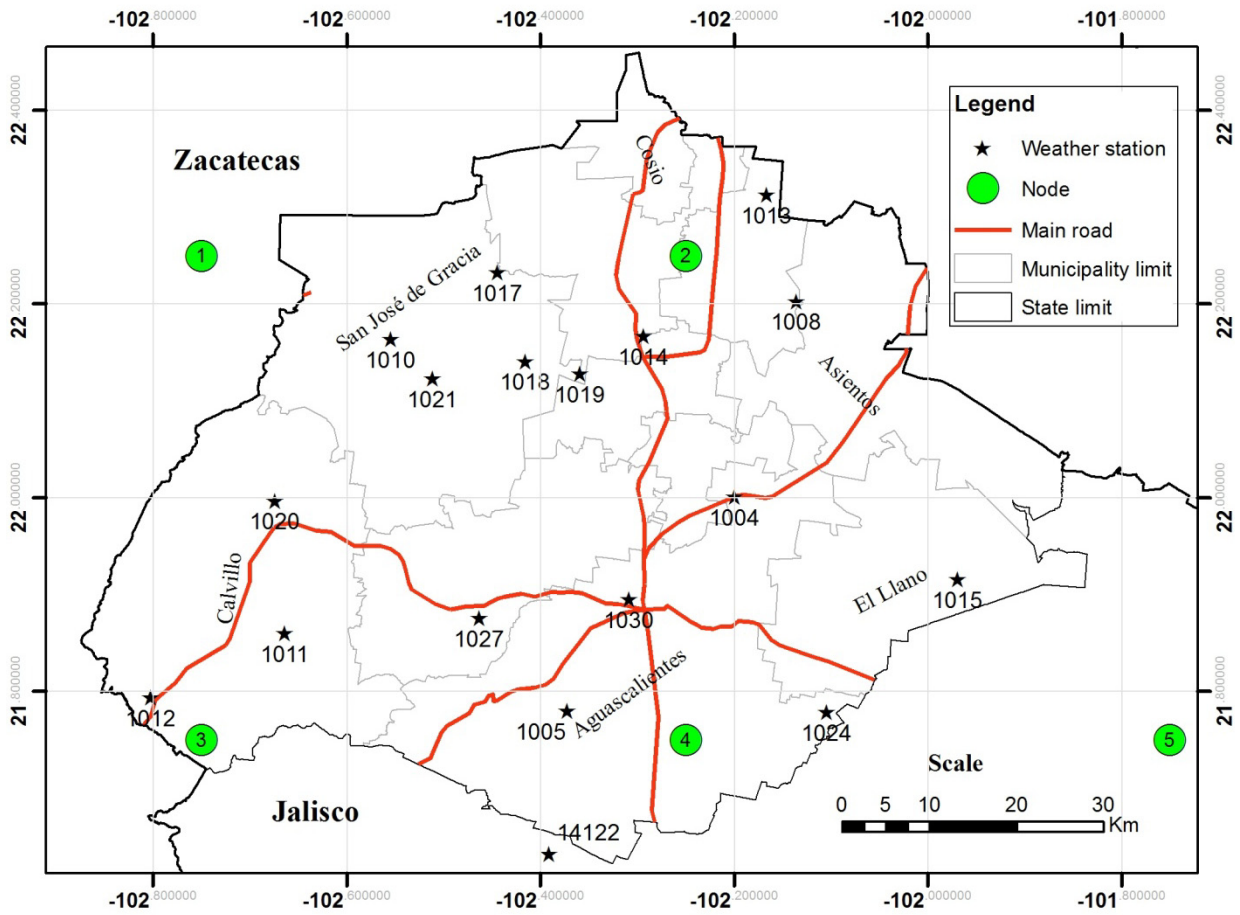

Figure 2. Spatial distribution of the WS-NWS and climate change nodes (50 x 50 km).

3.4.3. Climate change impact analysis

The technique used to analyze the impacts of climate change on soil erosion involved using *MAR* for historical values. Scenario A2 was used for the input values to determine the *GROPE* (Eq. 2) at a spatial distribution that was obtained via the IDW (Inverse Distance Weighting) method (this method has been used in similar studies [50,37]. This process allowed for the detection of local impacts once similar ranges had been adjusted for both the historical values and scenario A2 according to the method described by López-Santos et al. [37]. The anomalies of climatic change scenarios to A2 and A1B models, were used because they are closer to social and economic trend considerer to Mexico, both have been recommended and used in similar studies [31,33,40].

The relative importance of the changes for the three defined classes (high, medium, light) was obtained as follows:

$$RI_{ci} = \frac{S_{ci}*100}{\sum_{i=1}^{n} ci} \qquad \text{[Eq. 4]}$$

where *RIci* is the relative value (percentage) of the *i*-th defined class; *Sci* is the geospatial surface calculated from the *i-th* class; n is the number of defined classes; and $\sum_{i=1}^{n} ci$ is the sum of the surface of each class (*ci*) ranging from 1 to 3.

4. Results

As shown in Table 6, the historical standardized climatic dataset and the statistically downscaled dataset were analyzed using the mean annual temperature and rainfall values for each WS selected, and the anomalies for the A2 and AIB scenarios were determined. Both scenarios showed differences, but the most important difference concerned rainfall levels. The arithmetic average for the historical rainfall levels was 509 (± 83.1) mm. Thus, when A2 reported 2.2% (± 7.9) less rainfall than that in A1B, these rainfall levels were 8% (± 5.9%) higher. It is also important to note that for the negative standard deviation between the A2 and A1B scenarios, one is negative (−5.7%) while the other is positive (+2.5).

From this this brief comparison and given that the trends in Mexico reflect very heterogeneous patterns characterized by strong population growth and slow economic development and technological change, scenario A2 was used in this work.

4.1. The effects of climate change on key variables

The results of the analysis of the impacts of climate change on the main study variables (MAR, *GROPE*, *RAI*) are presented below.

4.1.1. Changes on mean annual rain

The changes in and effects of climate change on *MAR* were determined for both raster datasets. The raster images were segmented into equal ranges. Three comparable ranges were defined to analyze the changes in *HMAR* and MAR_{ScA2} (a1 vs. b1; a2 vs. b2; a3 vs. b3), thus clarifying the hazard magnitudes in terms of area. Positive and negative changes can thus be a "benefit or detriment" based on the variability of the data listed above (Table 6), which can manifest in future scenarios as class b1, the lower limit, or as class b3, the upper limit. For the first case, by averaging the *MAR* and given on the historical average of 509 mm for each class, we found that the increase in the future class b1 (MAR_{ScA2} b1) only reached 8.3 mm, while for class b3 (MAR_{ScA2} b3), the average rainfall reached 45.1 mm, denoting positive effects of 1.6 and 8.9%, respectively (Table 7).

The same comparative analysis between the classes (a1 vs. b1) shows that the MAR may increase by 19.5% in Aguascalientes when comparing the historical and future scenarios (2,039), changing from an area of 337.5 to 1,096.7 km^2. For classes b2 and b3, the following results were

observed: (1) The b2 class will maintain the same amount of rain (479 mm) but within an 11.4% smaller area than that observed for the historical scenario, changing from 3153.5 to 2510.2 km^2; and (2) the b3 class, with a 4.15 mm increase (+ 8.9%), will increase in area by equivalent of 35.8% of the total area of Aguascalientes (Table 7).

The spatial distributions of *HMAR* and PMA_{ScA2} (Figure 3) exhibit the following features:

(1) The *MAR* increase (1.7%) for the b1 class in scenario A2 was distributed across the north and southeast over 13.5% of the total area (5,621.5 km^2) of Aguascalientes. The municipalities of Cosío, Rincón de Romos and Tepezalá are located in the first (north) area, and the municipalities of Asientos, El Llano and Aguascalientes are located in the second (southeast) area.

(2) Although no increases are expected for MAR_{ScA2} in b2, we observed a decrease of 11.4% for the total study unit (SU) area, which in real terms indicates a reduced volume of water for municipalities located in the central area of the state (San José de Gracia, Jesús María, Pabellón de Arteaga and Aguascalientes) as well as in the east (portions of Tepezalá, Asientos and El Llano).

(3) Although there could be an *MAR* increase of 9.4% for the b3 class, this would be the result of a 2.1% smaller area than that observed in HMAR a3. The area to the west of the state corresponds to the municipalities of Calvillo, San José de Gracia, Asientos, San Francisco de los Romo and Aguascalientes.

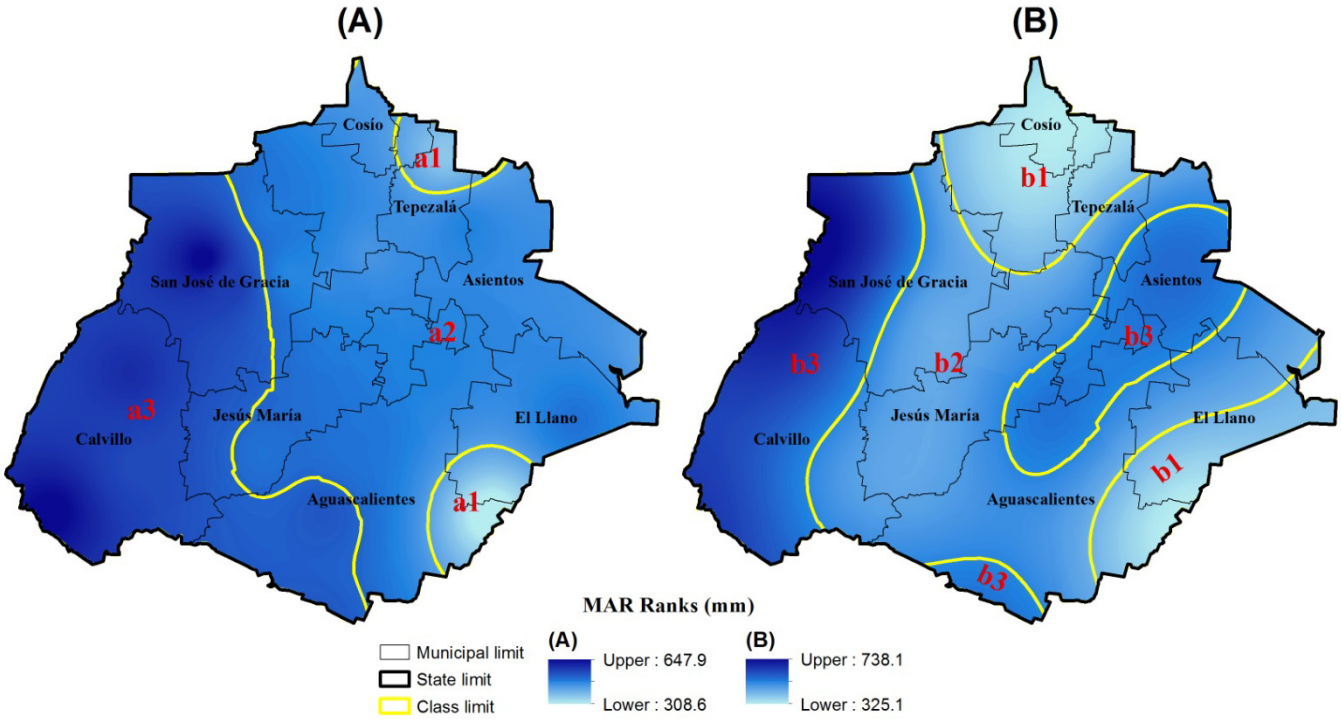

Figure 3. Spatial distributions of (A) *HMAR* and (B) MAR_{ScA2} in Aguascalientes.

Table 6. Mean annual historical rain and temperature levels and anomalies for A2 and A1B scenarios.

					MAR	**Anomaly**		***MAT***	**Anomaly**	
WS	Weather station	Location (lat/long)		masl	historical	A2	A1B	historic	A2	A1B
Code	*Official name*	*------ dg ------*		*m*	*mm*	*---- % ----*		*------- °C -------*		
1010	La Tinaja	22.164	102.554	2526	647.9	-4.9	4.4	16.7	1.7	1.8
1021	Rancho Viejo	22.123	102.511	2127	570.6	-10.7	7.5	18.2	0.3	0.3
1008	Pto. de la Concepción	22.203	102.135	2323	484.1	8.7	13.8	16.9	0.9	0.9
1013	Mesillas	22.313	102.166	2021	379.4	1.0	5.6	16.8	0.3	0.4
1014	Pabellón-Campo Exp.	22.167	102.293	1934	453.0	-6.4	3.3	15.3	0.6	0.6
1017	Presa Potrerillos	22.233	102.444	2172	495.0	-8.7	1.0	15.5	0.2	0.2
1018	Presa Calles	22.141	102.415	2053	478.3	-5.3	2.7	16.4	0.4	0.5
1019	Presa Jocoque	22.128	102.359	2006	469.2	-4.9	4.3	17.2	0.8	0.9
1011	Malpaso	21.860	102.664	1730	556.0	-8.1	3.7	20.7	0.2	0.1
1012	Presa Media Luna	21.794	102.802	1589	646.3	-2.5	2.2	15.5	0.8	0.8
1020	Presa la Codorniz	21.997	102.674	1850	594.6	4.1	8.6	18.7	0.9	1.0
1004	Cañada Honda	22.001	102.199	1925	486.3	10.3	17.4	17.3	0.8	0.9
1005	Presa El Niagara	21.780	102.372	1844	540.0	-7.2	2.6	17.6	0.7	0.4
1024	San Isidro	21.779	102.104	2004	308.6	8.5	13.6	15.3	0.8	0.8
1027	Venaderos	21.876	102.463	2026	505.8	-8.9	4.8	14.9	0.4	0.4
1030	Aguascalientes	21.895	102.308	1889	501.8	8.3	13.2	16.1	0.4	0.5
14122	San Bernardo	21.632	102.391	1085	540.1	4.6	18.1	15.6	0.4	0.5
1015	Palo Alto	21.916	101.969	2037	505.5	-16.6	17.4	17.1	1.0	1.1
			Average	*1952*	*509.0*	*-2.2*	*8.0*	*16.8*	*0.6*	*0.7*
			Stdev	*301*	*83.1*	*7.9*	*5.9*	*1.4*	*0.4*	*0.4*
			Max	*2526*	*647.9*	*10.3*	*18.1*	*20.7*	*1.7*	*1.8*
			Min	*1085*	*308.6*	*-16.6*	*1*	*14.9*	*0.2*	*0.1*

Table 7. Analysis of the probable effects of climate change on MAR in Aguascalientes for three comparable classes (*HMAR* vs. MAR_{ScA2}).

		----- MAR -----		***----- Analysis of changes and impacts -----***				
Variable	Class	Rank	Avg	FIC	PCR	Area	RPC	DBC
		---------- mm ----------			*%*	*km^2*	*----- % -----*	
HMAR	a1	308.6–437.7	373.2			337.5	6.0	
	a2	437.8–520.2	479.0			3 153.5	56.1	
	a3	520.3–647.9	584.1			2 130.5	37.9	
MAR_{ScA2}	b1	325.1–437.7	381.4	8.3	+1.6	1 096.7	19.5	+13.5
	b2	437.8–520.2	479.0	0	0	2 510.2	44.7	-11.4
	b3	520.3–738.1	629.2	45.1	+8.9	2 014.6	35.8	-2.1

FIC = Future Impact per Class (b1–a1; b2–a2; b3–a3); PCR = Proportion of Change in Rainfall (PCR = (FIC/509)*100); RPC = Relative Proportion per Class in % (RPC = (Area of class / Total Area)*100); DBC = Difference Between Classes (MAR_{ScA2}-*HMAR*); Avg = Average per class; the signs denote probable effects as positive (+) or negative (-) for the future scenario A2.

4.1.2. Changes in and effects on *GROPE* and *RAI*

The stratified analysis of the three comparable classes, as in the previous case for *GROPE* and RAI, shows consistencies in the spatial distribution of MAR. Both indices, from the relative to the historical, show that for the future scenario, the impact could be of the same magnitude because in the b1 class ($GROPE_{ScA2}$ b1 and RAI_{ScA2} b1), the impacts would reach 2.4 and 2.8%, whereas for the b3 class ($GROPE_{ScA2}$ b3 and RAI_{ScA2} b3), the increases could reach 13.2 and 15.3%, respectively (Table 8).

Table 8. Analysis of the probable impacts of climate change on the *GROPE* and RAI indices from three comparable classes.

		----- Impact -----					***----- Impact -----***			
Var	Class	Rank	Avg	IC	PFC	Var	Rank	Avg	FIC	PFC
		-------- Index --------			*%*		*-------- Index --------*			*%*
HGROPE	a1	41.2–72.2	56.7				36.5-75.1	55.8		
	a2	72.3–92.2	82.2			*HRAI*	75.2-99.8	87.5		
	a3	92.3–122.9	107.6				99.9-138.1	119		
$GROPE_{ScA2}$	b1	45.2–72.2	58.7	2.0	+2.4		41.4-75.1	58.25	2.45	+2.8
	b2	72.3–92.2	82.2	0	0	RAI_{ScA2}	75.2-99.8	87.5	0	0
	b3	92.3–144	118.4	10.8	+13.2		99.9-165.1	132.5	13.5	+15.4

Avg = Average; Var = Variable; FIC = Future Impact per Class (b1–a1; b2–a2; b3–a3); PFC = Proportion of Future Change (PFC = (FIC/AHV) * 100), AHV = Average for the Historical Variable (AHV = 82.1).

4.2. Description of the input variables in the erosion model

Our analysis of the relative importance and spatial distribution of the erosion model input variables (Eq. 3) reveals the gradient of soil susceptibility for the territory of Aguascalientes, as shown below.

4.2.1. *CAERO* Index

The *CAERO* index, which denotes the degree of soil susceptibility to the erosive effects of rain, exhibits the following degree of relative importance and spatial distribution (Figure 4a):

(1) Forty-six percent of the soils in Aguascalientes has a *CAERO* index of 2, demonstrating a high susceptibility to water erosion, as these soils are associated with the following soil groups: Calcisol (CL), Durisol (DU), Leptosol (LP) and Planosol (PL). These soil groups correspond to the municipalities of Jesús María, San José de Gracia and Pabellón de Arteaga. For the northeastern part of the state, these soil groups correspond to the municipalities of Cosío, Tepezalá, Asientos and part of the municipality of El Llano.

(2) In contrast, 32% of the territory had a *CAERO* index of 0.5, representing a low susceptibility to erosion in places where only the Phaeozem (PH) soil group was identified. This index (*CAERO*) value is distributed along the central-southern area of the state, including the municipalities of Aguascalientes, San Francisco de los Romo, Jesús María, El Llano and Calvillo.

(3) Finally, 18% of the territory had a *CAERO* index of 1, indicating a moderate susceptibility to erosion, and the following soil groups were identified: Cambisol (CM), Fluvisol (FL), Kastanozem (KS), Luvisol (LV), and Regosol (RG). This CAERO value was distributed in the western part of the state in the municipalities of Calvillo, San José de Gracia and Rincón de Romos; for the eastern area, this CAERO value was distributed in the municipalities of San Francisco de los Romo, Aguascalientes, El Llano and Asientos.

4.2.2. CATEX index

The *CATEX* index denotes the gradient of soil resistance to erosion processes associated with dispersion, flow formation and sedimentation. The relative importance and spatial distributions (Figure 4b) of this index are described below:

(1) Most of the territory of the state (82.8%) has a *CATEX* value of 0.3 because the soils have a fine texture (class 2), denoting a moderate susceptibility to erosion. This *CATEX* value extends over almost the entire territory, excluding certain central and southwestern areas.

(2) A *CATEX* value of 0.5 was assigned to 10.9% of the territory due to the presence of a stony or rocky phase denoting high susceptibility to erosion. This *CATEX* value is distributed across the southwestern area of the state (including the municipalities of Calvillo and Jesús María)

and across the eastern area (in the municipalities of El Llano, Asientos and San José de Gracia).

(3) Finally, 3.27% of the territory presented a *CATEX* value of 0.2 due to the presence of coarse soils (class 1) (which are highly susceptible to erosion). Territories with this value were found to be distributed in the central area of the state across the municipalities of Jesús María, Pabellón de Arteaga, San José de Gracia and Rincón de Romos.

4.2.3. CATOP index

The topographic properties of the study area proved to be very useful as they allowed us to identify areas where slope conditions and ground discontinuities determine erosion susceptibility, as described below:

(1) A *CATOP* index of 0.35 was assigned to 60% of the state territory because this area includes valleys, which are less susceptible to erosion. This *CATOP* value is distributed from the central to the eastern part of the state in the municipalities of Cosío, Rincón de Romos, Tepezalá, Pabellón de Arteaga, Asientos, Jesús María, San Francisco de los Romo, Aguascalientes y El Llano (Figure 4c).

(2) A *CATOP* index of 3.5 was assigned to the 27.4% of the area, denoting a moderate susceptibility to erosion. This area is mainly distributed in the western region of the state in the municipalities of Cosío, Rincón de Romos, San José de Gracia, Calvillo, Jesús María and Aguascalientes, and in the eastern area in some parts of the municipalities of Tepezalá, Asientos and El Llano (Figure 4c).

(3) Finally, 12.5% of the state territory is classified with a *CATOP* value of 11 due to the presence of sierras and falls, which are highly susceptible to erosion. This *CATOP* value is found in the same municipalities as the *CATOP* value of 3.5 (Figure 4c).

4.2.4. CAUSO index

The *CAUSO* index evaluates erosion susceptibility levels based on land use in Aguascalientes for 2010, and the results (Table 10) are as follows:

(1) With a *CAUSO* index of 0.3, 23.5% of the territory includes grasslands, denoting a moderate susceptibility to erosion. This *CAUSO* value is distributed across the central area of the state in the municipalities of Cosío, San José de Gracia, Jesús María and Aguascalientes (Figure 4d).

(2) In Aguascalientes, 22.5% of the land has a *CAUSO* index of 0.2, and because this land is utilized for irrigated agriculture, it exhibits a moderate susceptibility to erosion. This *CAUSO* value is distributed over the central area of the territory in the municipalities of Cosío, Rincón de Romos, Tepezalá, Pabellón de Arteaga, San Francisco de los Romo, Jesús María and Aguascalientes as well as in the southwest in Calvillo (Figure 4d).

(3) In total, 21.7% of the State of Aguascalientes has a *CAUSO* index of 0.7, and this land is

used for rainfed agriculture, denoting a high susceptibility to erosion. This *CAUSO* value is focused in the eastern part of the state in the municipalities of Tepezalá, Asientos and El Llano (Figure 4d).

(4) Forested areas cover 16.6% of the state, representing a *CAUSO* value of 0.1 and indicating a low susceptibility to erosion. These areas are distributed across the western part of the state in the municipalities of San José de Gracia, Calvillo and Jesús María.

(5) Scrubland, which covers approximately 12% of the land in Aguascalientes, has a *CAUSO* value of 0.15, denoting a low susceptibility to erosion. These areas are distributed across the northern and central areas of the state in the municipalities of Tepezalá, Asientos, Pabellón de Arteaga, San Francisco de los Romo and San José de Gracia and in the southwestern area in the municipality of Calvillo.

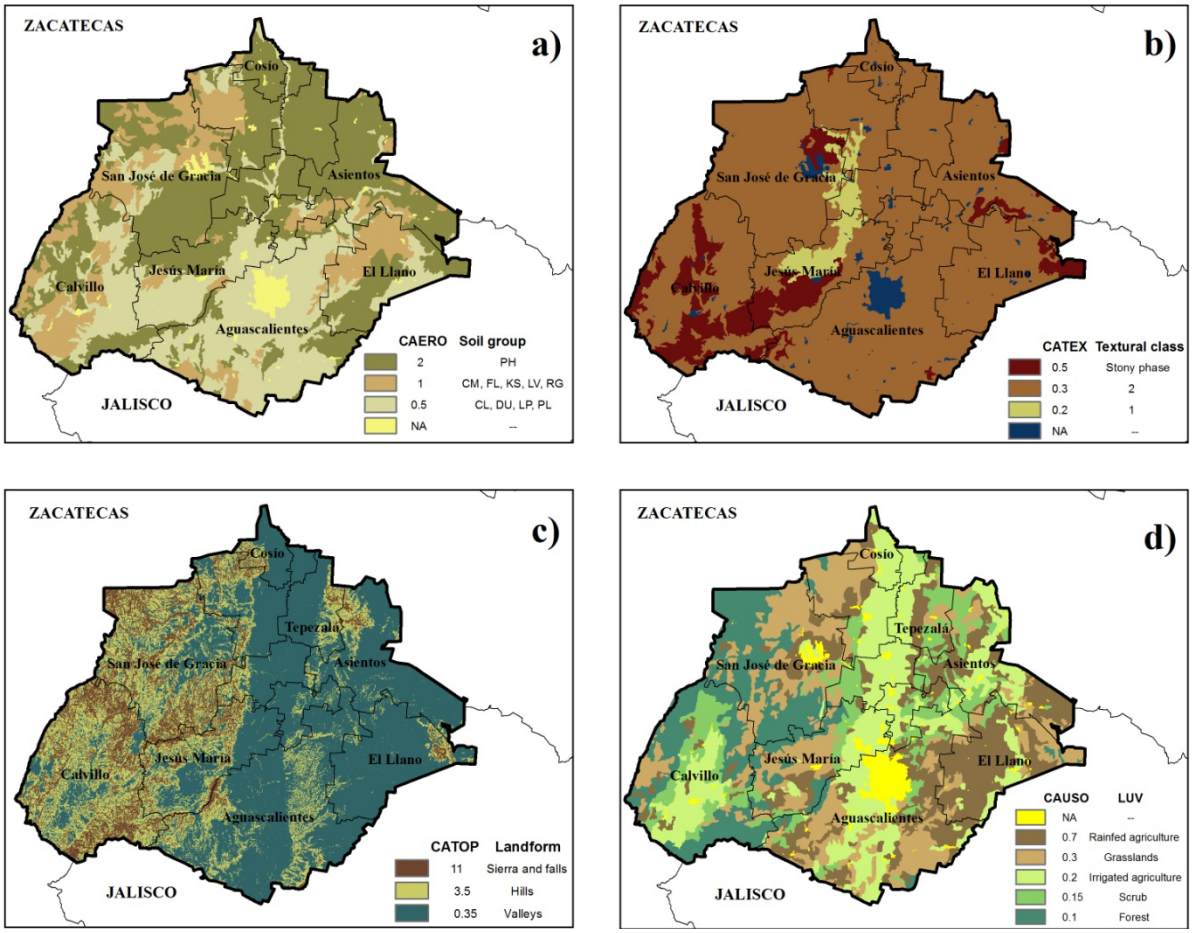

Figure 4. Spatial distribution of the (a) *CAERO*, (b) *CATEX*, (c) *CATOP* and (d) *CAUSO* indices for Aguascalientes.

4.3. Estimating the effects of climate change on LWE

The effects of climate change on *LWE* were estimated based on the input variables described above (3.1 and 3.2). Once transformed from vector files (*shp*) into raster images (vector ↔ raster),

these input variables were used to calculate the soil erosion rates in the study area based on the raster calculator available in ArcGIS 10.1 (Spatial Analyst). The results are described below (Table 9).

Table 9. Analysis of changes in and effects of the *LWE* on the study area for four comparable classes between historical and future A2 scenarios.

Erosion	*Class*	*Rank*	*Avg*	*FIC*	*PFC*	*Area*	*FCT*	*PFCT*
		------- *t ha^{-1} yr^{-1}* -------			*%*	---- *km^2* ----		*%*
HLWE	a1	0–10	5			3 110.8		
	a2	10–50	30			1 707.5		
	a3	50–200	125			766.9		
	a4	200–558.6	379.3			36.3		
LWE_{ScA2}	b1	0–10	5	0		3 211.8	+ 101	+ 1.8
	b2	10–50	30	0		1 639.1	- 68.4	- 1.2
	b3	50–200	125	0		724.8	- 42.1	- 0.8
	b4	200–750.7	475.4	96.1	34.4	45.8	+ 9.5	+ 0.2

AHV = Average of the Historical Variable (279.3 t ha^{-1} yr^{-1}); Avg = Average; FIC = Future Impact per Class (b1–a1; b2–a2; b3–a3; b4–b4); PFC = Proportion of Future Change (PFC = (FIC/AHV)*100); FCT = Future Change for the Territory; PFCT = Proportion of Future Change for the Territory (PFCT = FCT*100)/5 621.5); 5,621.5 km^2 = total study unit area.

(1) The average of the historical LWE variable was 279.3 t ha^{-1} yr^{-2}, and the variable ranged between the minimum (0 t ha^{-1} yr^{-2}) and maximum (558.6 t ha^{-1} yr^{-2}) values shown above (Table 9).

(2) Changes in the soil water erosion rates between the historical values and scenario A2 (*HLWE* and *LWE_{ScA2}*) are not evident, with the exception of class 4, which presents an estimated increase of 192.1 t ha^{-1} yr^{-1}. This value is equivalent to 34.4% of the average historical laminar water erosion (HLWE) value, which changes from 558.6 to 750.7 t ha^{-1} yr^{-1}.

(3) A decrease of 110.5 km^2 was estimated in the spatial distribution of classes 2 and 3 (moderate and high, respectively), representing 2% of the total area of Aguascalientes.

(4) Inversely, for classes 1 and 4, an increase of 110.5 km^2 was estimated. Class 1 will increase by 101 km^2, and class 4 will increase by 9.5 km^2.

In the SU, the spatial distribution of soil erosion susceptibility for the four analyzed classes is described in the following paragraph and in Figure (Figure 5).

Classes 1 and 2 (light and moderate, respectively) are located in all the municipalities of the state, mainly in the central and eastern regions. The municipalities covered by class 3 are mainly located in the west (Cosío, San José de Gracia, Calvillo, Jesús María) and in parts of the east (Tepezalá, Asientos and El Llano). Class 4 (very high) is found primarily in San José de Gracia, Calvillo, El Llano and Asientos.

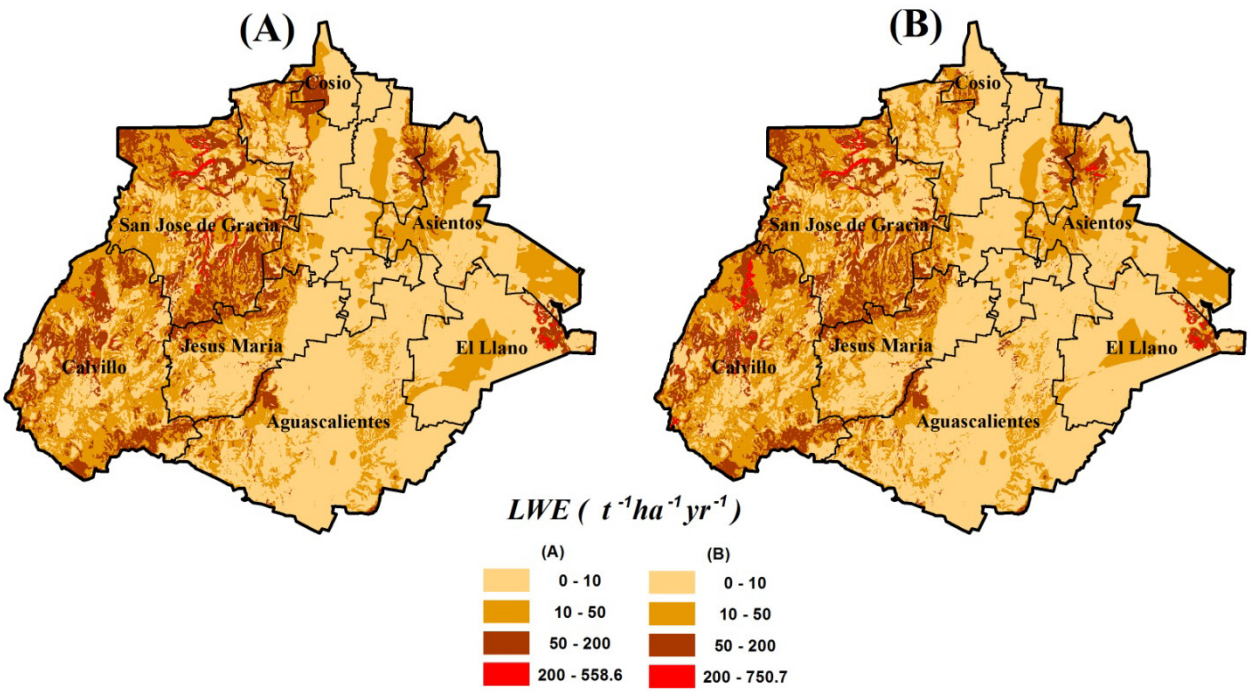

Figure 5. ***LWE*** **changes in spatial distribution between historical values (A) and future scenario A2 (B) for Aguascalientes.**

5. Discussion

Analysis of the local impacts of climate change on MAR and LWE

Rain variability in Aguascalientes is determined by El Niño (EN), La Niña and the EN/southeast oscillation (ENSO), with the main effects derived from the Pacific [51,52]. When these phenomena are combined with orographic variations, they produce arid and semiarid climatic gradients with rainfall levels of over 300 mm and up to 700 mm, respectively [53].

Magaña et al. [51] have argued that the occurrence and characteristics of ENSO can modify global climate patterns. During the winter ENSO in Mexico, these features increase precipitation in the northeast, while in the summer, they produce negative precipitation anomalies over much of Mexico. These results complement those of Pavia et al. [55], who analyzed data collected from approximately one thousand climatic stations across Mexico.

Among the erosion rates resulting from the calculations (Table 9), class 4 is classified in this case as very high, with an average value around of 475 t ha^{-1} yr^{-1} for the A2 scenario. This value is equivalent to an annual loss of approximately 0.30 mm of lamina considering a bulk density of 1.2 t m^{-3}. This means that while the future area of this class could be 9.5 km^2 (36.3–45.8 km^2), due to *MAR* changes in mountainous areas, as was shown before (Figure 4c), the risks could be more significant due the natural processes described above. Areas without official protection plans [19,20] could

experience irreversible land degradation beyond that described here.

In reference to similar areas (arid, semiarid and subhumid) as those examined this study show erosion rates almost same [26–28]. For example, Zhang et al. [26] in northwestern Shanxi Province in the Loess Plateau area of China, used the RUSLE model to find high soil erosion rates (> 500 t ha^{-1} yr^{-1}) in areas presenting significant terrain alterations, high slopes, and land with sparse vegetation. The authors show that hilly areas, grasslands, and newly constructed mine dumping areas are more degraded and have higher levels of erosion. However, in some cases, reversing these impacts is possible, as described by Jiao et al. [56] for the Yellow River Basin, which is located in the Shanxi and Shaanxi provinces in China.

Chaplot [27] reported the same erosion rates by modeling variations in rainfall in SWAT (Soil and Water Assessment Tool) for a watershed located in Central Texas (Waco) with similar conditions as part of the SU described above (Figure 4c, 4d). In other words, for class 4, which corresponds to areas with forest vegetation in the upper parts of the west of Aguascalientes, there are high erosion rates (> 475 t ha^{-1} yr^{-1}) resulting in a soil loss of 0.3 mm (0.0003 m yr^{-1}).

The effects of the soil losses that could occur in the near future (2010–2039) are more significant than those reported by Montes-León et al. [24]. Extreme potential erosion (> 250 t ha^{-1} yr^{-1}) has been estimated for Hydrologic Region No. 12 (RH12), which comprises the hydrologic system of Lerma-Santiago, where Aguascalientes is located. This result is considered a possibility for the following three reasons: 1) the rate of extreme erosion is not the exact upper limit of the range; 2) areas with undulating terrain that are poorly managed and that are subject to torrential seasonal rains are generally more susceptible to erosion; and 3) studies on similar environments that do not consider the effects of climate change have reported erosion rates of up to average cited here (475 t ha^{-1} yr^{-1}) according to the USLE and others models [23,26–28].

6. Conclusions

Soil loss represents the initial state of environmental degradation in the SU. According to previous studies, soil loss is likely an underestimated problem, as these studies have not examined climate scenarios with different rain and LWE spatial distributions as principal variables for both the present and the future.

The calculated rate of water erosion shows that for the future scenario LWE_{ScA2} (2010–2039), if soil erosion is not addressed through policies, prevention practices, conservation and the protection of natural resources, the soil layer that currently performs fundamental stabilizing functions in ecosystem services and that represents an income source related to primary activities could be lost. While the impacts described here, which are based on annual soil loss rates and climatic seasonal (dry and wet) effects, are not yet clear, we present a good approximation according to the scientific references discussed.

A more comprehensive understanding of this issue is desirable for applying the new climate

change scenarios (RCP 5) proposed in the IPCC's Fifth Assessment Report.

Acknowledgments

This research was conducted as part of the Chapter Vulnerability Studies of Natural Resources to Climate Change project with support from the State Program of Climate Change of Aguascalientes (PEACC-Ags, Spanish acronym) and SEMARNAT-CONACYT sectorial funds (clave: S0010–2008).

Conflict of interest

Both authors declare no conflicts of interest in this paper.

References

1. Sun W, Shao Q, Liu, J, et al. (2014) Assessing the effects of land use and topography on soil erosion on the Loess Plateau in China. *Catena* 121: 151-163.
2. Stavi I, Lal R (2015) Achieving zero net land degradation. *J Arid Environ* 112: 44-51.
3. Zhao Q, Li D, Zhuo M, et al. (2015) Effects of rainfall intensity and slope gradient on erosion characteristics of the red soil slope. *Stoch Environ Res Risk Assess* 29: 609-621.
4. Wang Y, Zhang JH, Zhang ZH, et al. (2016) Impact of tillage erosion on water erosion in a hilly landscape. *Sci Total Environ* 551-552: 522-532.
5. UNCCD (2013) Economic assessment of desertification, sustainable land management and resilience of arid, semi-arid and dry sub-humid areas. 1 Eds., Global Risk Forum GRF Davos & United Nations Convention to Combat Desertification.
6. Ferreira V, Panagopoulos T (2014) Seasonality of soil erosion under mediterranean conditions at the Alqueva dam watershed. *Environ Manage* 54: 67-83.
7. López-Santos A (2016) Neutralizar la degradación de las tierras, una aspiración global. ¿es posible lograrlo en México? Terra Latinoamericana 34: 239-249.
8. Nielsen UN, Ball BA (2015) Impacts of altered precipitation regimes on soil communities and biogeochemistry in arid and semi-arid ecosystems. *Global Change Biol* 21: 1407-1421.
9. Polyakov VO, Nearing MA, Stone JJ, et al. (2016) Quantifying decadal-scale erosion rates and their short-term variability on ecological sites in a semi-arid environment. *Catena* 137: 501-507.
10. Gao X, Xie Y, Liu G, et al. (2014) Effects of soil erosion on soybean yield as estimated by simulating gradually eroded soil profiles. *Soil Tillage Res* 45: 126-134.
11. Nkonya E, Gerber N, Baumgarther P, et al. (2011) The economics of land degradation. Toward an integrated global assessment. 1 Eds., Peter Lang International Verlag der Wissnschaften, serie 66.
12. Gnacadja L (2012) Zero net degradation. A sustainable development goal for Rio+20. 1 Eds.,

United Nations Convention to Combat Desertification. Available from: http://www.unccd.int/Lists/SiteDocumentLibrary/Publications/ZNLD%20Summary%20final.pdf.
13. Garrido A, Cotler H (2010) Degradación de suelos en las cuencas hidrográficas de México. In Cotler H, et al, Las Cuencas Hidrográficas de México. 1 Eds., Secretaría del Medio Ambiente y Recursos Naturales: 104-107.
14. SEMARNAT (2011) Estrategia nacional de manejo sustentable de tierras. 1 Eds., Secretaría de Medio Ambiente y Recursos Naturales: 160.
15. CONAFOR-UACh (2013) Línea base nacional de degradación de tierras y desertificación. Informe final. Comisión Nacional Forestal & Universidad Autónoma Chapingo: 161.
16. SEMARNAT-INECC (2012) Quinta Comunicación Nacional ante la Convención Marco de las Naciones Unidas sobre el Cambio Climático. 1 Eds., Secretaría de Medio Ambiente y Recursos Naturales & Instituto Nacional de Ecología y Cambio Climático: 441.
17. Lal R (2001) Soil degradation by erosion. *Land Degrad Dev* 12: 519-539.
18. Cotler AH (2003) Características y manejo de suelos en ecosistemas templados de montaña. Instituto Nacional de Ecología, in Sánchez O., E. Vega, E. Peters y O. Monroy-Vilchis Publishers, *Conservación de ecosistemas templados de montaña en México.* 1 Eds. INE-SEMARNAT, Mexico, 153-161.
19. IMAE (2005) Programa Estratégico Forestal del Estado de Aguascalientes, Visión 2030. 1 Esd., Instituto del Medio Ambiente del Estado de Aguascalientes. Avalilable from: http://www.conafor.gob.mx:8080/documentos/download.aspx?articulo=174.
20. SEMARNAT (2008) Informe de la situación del medio ambiente en México. Compendio de estadísticas ambientales. Secretaría de Medio Ambiente y Recursos Naturales. 1 Eds., Secretaría de Medio Ambiente y Recursos Naturales: 380.
21. Pacheco-Martínez J, Cabral-Cano E, Wdowinski S, et al (2015) Application of InSAR and gravimetry for land subsidence hazard zoning in Aguascalientes, Mexico. *Remote Sens* 7: 17035-17050.
22. Aranada-Gómez JJ (1989) Geología preliminar del graben de Aguascalientes. Rev. *Mex Cienc Geol* 8: 22-32.
23. Cardona MA, Colmenero JAR, Valderrábano MLA (2007) La erosión hídrica del suelo en un contexto ambiental en el Estado de Tlaxcala, México. *Ciencia Ergo Sum-UAEM* 14: 317-326.
24. Montes-León MA, Uribe-Alcantara EM, García-Celis E (2011) Mapa de erosión potencial. Tecnología y Ciencias del Agua 2: 5-17.
25. Jang Ch, Shin Y, Kum D, et al. (2015) Assessment of soil loss in South Korea based on land-cover type. *Stoch Environ Res Risk Assess* 29: 2127-2141.
26. Zhang L, Bai KZ, Man J, et al. (2016) Basin-scale spatial soil erosion variability: Pingshuo opencast mine site in Shanxi Province, Loess Plateau of China. *Nat Hazards* 80: 1213-1230.
27. Chaplot V. (2007) Water and soil resources response to rising levels of atmospheric CO_2 concentration and to changes in precipitation and air temperature. *J Hydrol* 337: 159-171.
28. Bera A. (2017). Estimation of soil loss by USLE model using GIS and remote sensing

techniques: a case study of Muhuri River Basin, Tripura, India. *Eurasian J Soil Sci* 6: 206-215.

29. Moss RH, Edmonds J. A, Hibbard KA (2010) The next generation of scenarios for climate change research and assessment. *Nature* 463: 747-756.
30. DOF (2013) Ley General de Cambio Climático. Cámara de Diputados. Available from: http://www.diputados.gob.mx/LeyesBiblio/pdf/LGCC_010616.pdf.
31. Conde AAC, Gay GGC (2008) Guía para la generación de escenarios de cambio climático a escala regional. Centro de Ciencias de la Atmósfera-UNAM. Available from: http://www.atmosfera.unam.mx/cclimat/Taller_CCA_INE_dic08/Guia_escenarios.pdf.
32. IPCC (2007) Climate Change 2007: The Physical Science Basis. Contribution of Working Group I to the Fourth Assessment. Report of the Intergovernmental Panel on Climate Change [Solomon, S., D. Qin, M. Manning, Z. Chen, M. Marquis, K.B. Averyt, M. Tignor and H.L. Miller (eds.)]. Cambridge University Press, Cambridge, United Kingdom and New York, NY, USA: 996.
33. Conde C, Estrada F, Martínez B, et al. (2011) Regional climate change scenarios for México. *Atmósfera* 24: 125-140.
34. INEGI (2012) Anuario estadístico y geográfico de Aguascalientes 2015. Available from: http://www.beta.inegi.org.mx/app/biblioteca/ficha.html?upc=702825076115.
35. INEGI (2007) Conjuntos de datos vectoriales de la serie IV de Uso de Suelo y Vegetación para la cobertura de Aguascalientes, México, escala 1:250 000. Available from: http://www.inegi.org.mx/geo/contenidos/recnat/usosuelo/Default.aspx.
36. SEDESOL-INE (1998) Ordenamiento ecológico del territorio. Memoria técnica metodológica. 1 Eds., Secretaria de Desarrollo Social & Instituto Nacional de Ecología: 66.
37. López-Santos A, Pinto JE, Ramírez EML, et al. (2013) Modeling of the potential impact of climatic change using two environmental indicators in northern Mexico. *Atmósfera* 26: 479-498.
38. López-Santos A, Martinez-Santiago S (2015) Use of two indicators for the socio-environmental risk analysis of Northern Mexico under three climate change scenarios. *Air Qual Atmos Health* 8: 331-345.
39. Ortiz-Solorio CA (1987) Elementos de agrometeorología cuantittiva con aplicaciones en la República Mexicana. 1 Eds., Universidad Autónoma Chapingo: 327.
40. Monterroso RAI, Conde AC, Rosales DG, et al. (2011) Assessing current and potential rainfed maize suitable under climate change scenarios in Mexico. *Atmósfera* 21: 53-67.
41. UNCCD (2012) Desertification, a visual syntesis. 1 Eds., Christina Stuhberg & Otto Simonett Yukie Hori. United Nations Convention to Combat Desertification & Zoi Environment Network. Available from: http://www.unccd.int/Lists/SiteDocumentLibrary/Publications/Desertification-EN.pdf.
42. Wischmeier WH, Smith DD (1978) Predicting rainfall erosion losses. A guide to conservation planning. USDA Agricultural Handbook, vol 537.
43. Morgan RPC (2005) Soil erosion and conservation. 3 Eds., Blakwel Publishing. National Soil Resources Institute, Cranfield University: 312.

44. IUSS-WG-WRB (2015) World reference base for soil resources 2014. International soil, update 2015 classification system for naming soils and creating legends for soil maps. World soil resources Reports No. 106. Roma, FAO: 203.
45. INEGI (2004) Guía para la interpretación de cartografía. Edafología, serie I. 1 Eds., Instituto Nacional de Estadística, Geografía e Informática: 27.
46. INEGI (2007) Conjunto de datos vectoriales de la serie II de Edafología para la cobertura de Aguascalientes, escala 1:250,000. Available from: http://www.inegi.org.mx/geo/contenidos/recnat/edafologia/vectorial_serieii.aspx.
47. INEGI (2011) Guía para la interpretación de cartografía. Edafología, serie II. Instituto Nacional de Estadística, Geografía e Informática: 32.
48. INEGI (2002) Conjuntos de datos vectoriales de Uso de Suelos y Vegetación serie III, para la cobertura de Aguascalientes, México, escala 1:250,000. Available from: http://www.inegi.org.mx/geo/contenidos/recnat/usosuelo/inf_e1m.aspx.
49. INEGI (2014) Continuos de elevación del territorio mexicano 3.0. Datos de Relieve continental. Available from: http://www.inegi.org.mx/geo/contenidos/datosrelieve/continental/descarga.aspx.
50. Karaca F (2012) Determination of air quality zones in Turkey. *JAPCA J Air Waste Ma* 62: 408-419.
51. Magaña VO, Vázquez JL, Pérez JL, et al. (2003) Impact of El Niño on precipitation in Mexico. *Geofís Int* 42: 313-330.
52. Magaña RVO, Zermeño D, Neri C (2012) Cimate change scenarios and potential impacts on water availability in northern Mexico. *Clim Res* 51: 171-184.
53. Peralta-Hernández AR, Barba-Martínez LR, Magaña-Rueda VO, et al. (2008) Temporal and spatial behaivor of temperatura and precipitation during the canicula (mindsummer drought under El Niño conditions) in central Mexico. *Atmósfera* 21: 256-280.
54. Peralta-Hernádez AR, Barba-Martinez LR (2009) The risk of early frost in central Mexico under El Niño conditions. *Atmósfera* 22: 111-123.
55. Pavia EG, Graef F, Reyes J (2006) PDO-ENSO effects in the climate of Mexico. *J Clim* 19: 6433-6438.
56. Jiao JY, Wang Z, Zhao G, et al. (2014) Changes in sediment discharge in a sediment-rich region of the Yellow River from 1955 to 2010: implications for further soil erosion control. *J Arid Land* 6: 540-549.